Detection of building regions using airborne LiDAR – A new combination of raster and point cloud based GIS methods

Bernhard HÖFLE, Werner MÜCKE, Marieke DUTTER, Martin RUTZINGER, Peter DORNINGER

Abstract

In this paper, a new GIS workflow for fully automated building detection from airborne LiDAR data is introduced. The strengths of both raster and point cloud based methods are combined, in order to derive reliable building candidate regions serving as input for 3D building outline extraction and modeling algorithms. Input data are a normalized Digital Surface Model (nDSM) and a slope-adaptive echo ratio raster, which is a significant parameter for solid objects with low surface roughness, such as buildings. In contrast, high vegetation exhibits a local vertical distribution of laser echoes leading to a low echo ratio value. Potential building areas are detected in the raster domain using standard tools provided by GRASS GIS. Seed regions are identified by using a threshold on (i) object height >2.0 m and (ii) echo ratio >75%. The following growing of the seed regions provides that building walls, overhanging roof parts, and areas obstructed by high vegetation are included. Finally, non-building regions are removed by an object-based classification using a threshold on average laser point surface roughness. The presented candidate region detection achieves high completeness (>97%) with already moderate correctness (>70%). By applying an existing 3D building outline extraction and modeling algorithm, the applicability of the derived candidate building regions is demonstrated.

1 Introduction

High automation in data acquisition and processing for deriving 3D digital city models is of great interest for end-users. Additionally, driving factors are higher success rate and quality, which reduce manual interaction and therefore costs. This can be achieved by the development of workflows covering the whole process from raw data to final products. The utilization of Airborne LiDAR (Light Detection and Ranging), also referred to as Airborne Laser Scanning, for 3D topographic data acquisition has gained more importance in the last few years. In contrast to photogrammetric techniques, the active LiDAR technology allows a direct determination of 3D elevation information, less sensitive to cloud cover and shadows, and it also provides the capability to "see" through small gaps in vegetation, which is an obvious advantage, if the object of interest (e.g. building) is occluded by high vegetation (e.g. trees). The obtainable accuracy (<0.5 m horizontal and <0.2 m vertical) as well as the high sampling densities (>50 points/m^2), which have become operationally available, are additional reasons for using LiDAR in 3D city modeling (KAARTINEN et al. 2005).

The extraction of 3D building models comprises several steps (MAAS & VOSSELMAN 1999), such as (i) building detection and outline extraction, as well as (ii) building modeling.

Firstly, regions are identified, giving a coarse spatial representation of candidate areas containing buildings, in which a more precise building outline is derived. Secondly, building modeling aims at the three-dimensional geometrical reconstruction of the objects that have been detected in the previous step. If building outlines are already available, for example given by a digital cadastral map or manual digitization, the completeness, up-to-dateness as well as the object representation have to be checked before using it directly for building modeling. It has to be taken into account that a different object representation is given in cadastre and LiDAR data, as the cadastre mostly contains the building outline represented by the walls, whereas in LiDAR data the most exterior parts of the buildings (e.g. roofs) delineate the object. Several authors have shown that best results can be achieved by performing both building detection and modeling using airborne LiDAR data as primary data source (e.g. RUTZINGER et al. 2009, and references therein).

Full 3D support is only given in the original LiDAR point cloud, where even building parts occluded by vegetation are represented. LiDAR derivatives, such as the digital surface model, or aerial imagery do not allow detecting such obstructed areas. However, the arising data volume of dense point clouds, which are required for deriving high quality building models, is difficult to handle and demands for sophisticated data management and processing algorithms (HÖFLE et al. 2006). Dependent on the study site the building regions may cover only a certain percentage of the whole area and LiDAR data, respectively, where the remaining areas comprise terrain (e.g. roads, grass) and high vegetation (e.g. trees). This fact has been utilized by RUTZINGER et al. (2008) and led to the development of a combined raster and point cloud based analysis approach. Basically, the advantages of the raster domain (i.e. fast processing and simple data model) are used in a first step, in order to substantially reduce the area of interest and thus the remaining data volume of the point cloud. Thereafter, the final delineation and modeling of the objects detected in the raster domain are performed in the original 3D point cloud, providing the highest accuracy and the possibility to separate objects that are overlapping in 2D.

This paper presents a new method for automated building detection in airborne LiDAR data by development of a workflow combining a raster and point cloud based GIS analysis. The main focus is to find candidate building regions with full completeness, which serve as input for an existing point cloud based method for building outline detection and modeling, such as the method developed by DORNINGER & PFEIFER (2008). Automated building detection is a fundamental step, in order to achieve a comprehensive, fully operational workflow for 3D building model generation.

2 Study area and datasets

The study area is located in the city of Hohenems (Vorarlberg, Austria) and covers an area of 0.35 km^2. The selected area is characterized by a great variety of land cover types such as forest, agricultural land and infrastructure objects including roads, buildings and also power lines. The airborne LiDAR data were acquired under leaf-off conditions in November 2003 with an Optech ALTM 2050 system. The average point density is 3 echoes/m^2. From the point cloud, a Digital Terrain Model (DTM) with 1 m resolution is derived with the software SCOP++ (PFEIFER et al. 2001) using robust filtering ("Lidar Default Strong" strategy). The Digital Surface Model (DSM) is produced in GRASS GIS (modul *r.in.xyz*)

by simple rasterization of all laser points into a 0.5 m regular grid, where the maximum elevation is chosen as cell value. Isolated cells containing no laser point at all, obtain the median elevation value of the 5x5 cell neighborhood. By subtracting the DTM from the DSM the so-called normalized DSM (nDSM) with 0.5 m resolution is calculated, representing the relative object heights above the terrain. For evaluation, a Digital Cadastral Map (DCM) is available as reference dataset provided by the land survey office of Vorarlberg (LVA Feldkirch). Minor manual revision of the DCM is performed by removing small (<20 m^2) and low objects (<2.0 m) as well as buildings that have been pulled down and thus are not present in the LiDAR data.

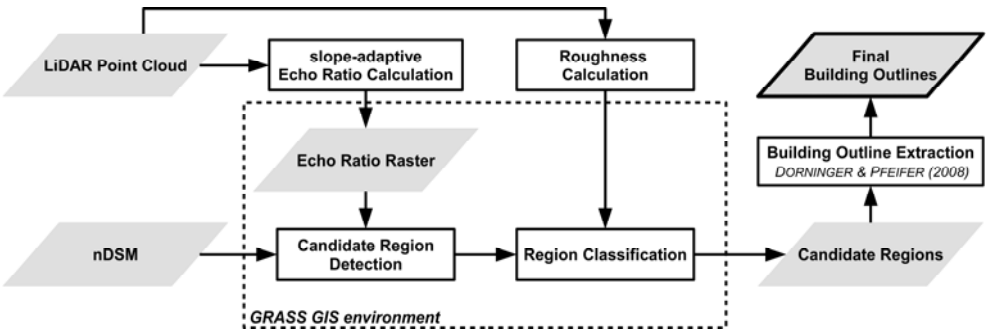

Fig. 1: The workflow of raster and point cloud based building candidate region detection implemented in the GRASS GIS environment with following point cloud based building outline extraction developed by DORNINGER & PFEIFER (2008)

3 Workflow

The fundamental concept is to find building candidate regions using a GIS based raster analysis for following point cloud based building outline detection and modeling within the detected regions. To cover all buildings, ensuring full completeness is favored over achieving full correctness because further classification and rejection of non-building candidate regions can be performed even better in the 3D point cloud, where also overhanging vegetation can be separated from roofs, which is not possible in the raster domain (e.g. nDSM, orthophoto). The developed workflow for building region detection is shown in **Fig. 1** and has been implemented in the GRASS GIS environment (GRASS DEVELOPMENT TEAM 2009). The major processing steps with intermediate results will be described in detail below.

3.1 Echo ratio raster derivation

3.1.1 Echo Ratio definition

As the nDSM includes all buildings but also raised non-building objects such as vegetation that exhibit a certain height above the terrain, the major task is to separate these objects in the nDSM by finding distinct parameters (i.e. raster layers) for buildings. A suitable pa-

rameter – a point density ratio – derived in the 3D point cloud was introduced by RUTZINGER et al. (2007), which they used for distinguishing vegetation from buildings. We call our modified version *Echo Ratio (ER)*, which is a measure for local transparency and roughness and is calculated in the 3D point cloud directly (**Fig. 2**). The *ER* is derived for each laser point and is defined as follows:

$$\textit{Echo Ratio}\ [\%] = n_{3D} / n_{2D} \cdot 100.0 \qquad \text{with } n_{3D} \leq n_{2D} \text{ and}$$

n_{3D}…number of points found in a fixed search distance (e.g. 1.0 m) measured in 3D (i.e. search sphere)
n_{2D}…no. of points found in same distance measured in 2D (i.e. vertical search cylinder with infinite height)

A good estimate for the selection of a suitable search distance is the double of the average point spacing found in the study area. This guarantees a representative number of neighbors, while avoiding too large neighborhoods, which would cause expanded transition zones at the border of two objects with different surface structure. A search distance of 1.0 m has been chosen for study area Hohenems. Buildings are assumed to have low transparency, which means that laser shots are not able to penetrate the surface (i.e. roof) and therefore are recorded at the surface only. In contrast, the laser beam is able to "see" through vegetation, which leads to recorded echoes in the canopy but also in the vertical profile (e.g. at branches and stems) and finally on the terrain. For roof areas the number of 3D and 2D neighbors should be approximately the same, resulting in a high *ER*, whereas the vertical distribution of laser points in vegetation results in a low *ER* value.

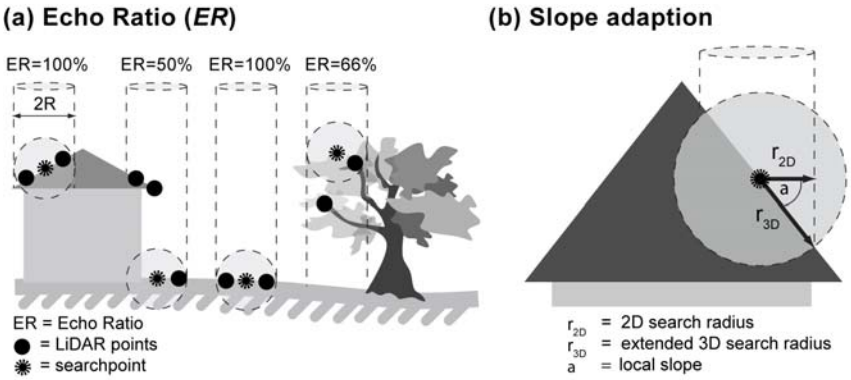

Fig. 2: (a) Point cloud based calculation of Echo Ratio (*ER*) for each laser point (i.e. search point) with example values for different landscape objects, and (b) slope adaption (i.e. extension of 3D search radius r_{3D}) dependent on slope for locally planar but slanted surfaces such as roof faces, with adjusted $r_{3D}=r_{2D} / cos(\alpha)$

3.1.2 Slope adaption

With increasing slope of the roof surface, even if the surface is fully solid, the *ER* gradually decreases. To guarantee a high *ER* on steep roofs, the 3D search distance has to be extended considering the roof slope. This is done by dividing the initial 3D distance by the cosine of the roof slope (**Fig. 3b**). We therefore call this parameter *slope-adaptive Echo Ratio* (*sER*).

This strategy of adaptive neighborhood search has also been used in a similar way by other authors (e.g. FILIN & PFEIFER 2006). The local slope estimation is done by fitting a plane minimizing the vertical residuals to the neighbors found in the initial 3D neighborhood. If plane fitting is successful (e.g. $n_{3D} \geq 3$) and the standard deviation of residuals does not exceed a certain threshold (e.g. <0.5 m), which stands for the planarity and smoothness of the local region, n_{3D} is recounted by using the extended search radius and *sER* replaces the standard *ER* value. Otherwise the search point lies most probably within vegetation where no reliable local plane can be estimated, and hence the *sER* is set to the *ER* value. Once *sER* has been derived for each laser point, an echo ratio raster layer (0.5 m cell size) is derived by aggregation of the values into regular cells using the GRASS GIS module *r.in.xyz*. The minimum *sER* value is taken per cell, in order to remove vegetation areas as good as possible. In roof areas without objects (e.g. antennas) and no roof overhang the *sER* value obtains 100%, whereas vegetation exhibits considerably lower values (**Fig. 3**).

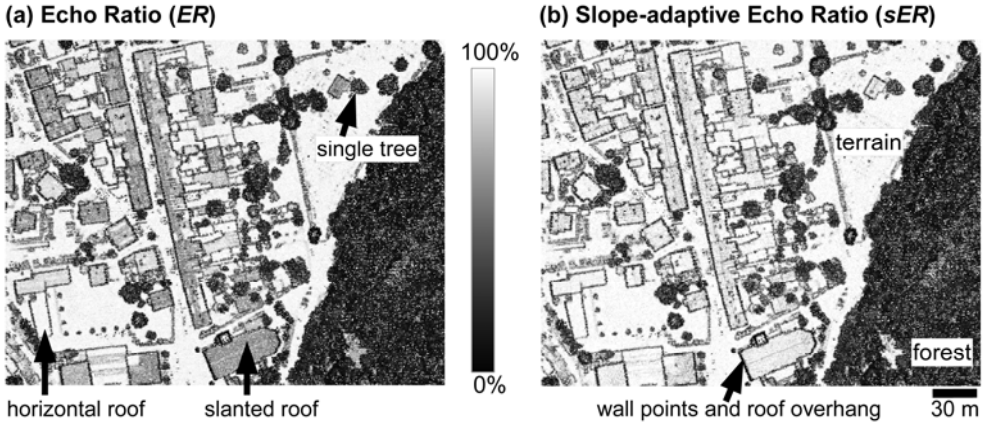

Fig. 3: Derived Echo Ratio images (0.5 m cell size; minimum value) with improvement from slope consideration in slanted roof areas shown in subfigure (b)

3.2 Detection of candidate regions

As input for the detection of candidate building regions the nDSM and the derived *sER* raster are used. In order to remove the terrain (i.e. bare Earth), which can also be seen as solid object with high *sER* values, and to remove vegetation, thresholds on nDSM and *sER*, respectively, are applied (**Fig. 4a**). Building regions are defined to lie >2.0 m above the terrain and to exhibit a *sER* value >75%, which has been found by investigation of the *sER* values within the buildings represented in the digital cadastral map. After the classification of the input datasets a mode filter in a 3x3 cells moving window is applied to the binary raster, which has value 1 for buildings and value 0 for non-building. The mode filter assigns small isolated pixels/pixel groups to the dominating class of the local window. This suppresses the "salt & pepper" effect originating from very small objects (e.g. antennas) and closes small gaps in the vegetation. Then cells are grouped to single regions with unique ID that form physically discrete areas (GRASS module *r.clump*). Thereafter, clumped areas smaller than 5.0 m^2 are removed because these small areas mainly comprise

dense crowns of trees, which have a high *sER*. The resulting areas represent roofs (**Fig. 4b**), but without small dormers, chimneys, as well as building parts covered by high vegetation and areas where roofs overhang each other or the terrain and the *sER* drops below the specified 75%. To include these missing building parts in the final building region approximation, the single regions are grown simultaneously to a maximum distance of 4.0 m (GRASS module *r.grow*), but restricted to areas >2.0 m above the terrain. This ensures that previous holes in the roofs are closed and that roof overhangs are attached to the existing regions if their excess length does not exceed the chosen growing distance. The final building region raster layer is then converted to a polygon vector, where each detected building region is represented by a polygon.

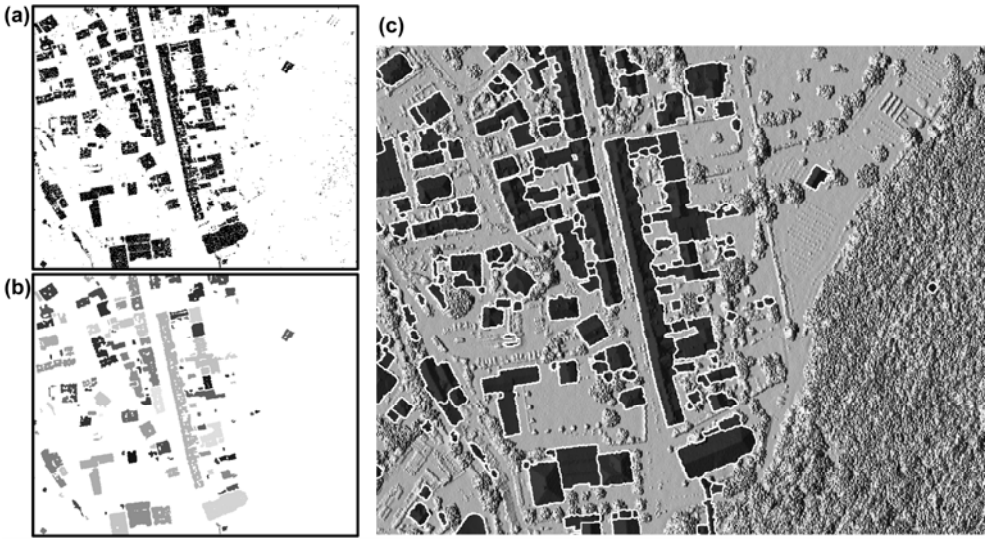

Fig. 4: (a) Areas fulfilling the thresholds on nDSM >2.0 m and *sER* >75.0%, (b) potential building areas after mode filtering, grouping of distinct connected regions and removal of small areas (<5.0 m^2), and (c) shading of nDSM overlaid with the final building candidate polygon layer.

3.3 Object-based classification

The classification aims at removing non-building regions that can be identified by using significant object-based features. Dense vegetation with a surface having low elevation variation (i.e. roughness within a smaller scale than the *ER* search radius) is very similar to a building object regarding the geometrical appearance in the LiDAR data. But in a smaller scale the surface roughness of vegetation regions exhibits higher average values compared to buildings. Exceptions are large, dense hedgerows with a planar surface, which can hardly be separated by using geometrical information only. The fact that non-building regions have a significantly higher average surface roughness is utilized in an object-based classification of the candidate regions.

Local roughness is calculated in the point cloud and estimated from the eigenvalues of the covariance matrix of fitting a local regression plane to the *k* nearest neighbors in 3D (k=32 for our study site) where fifty percent plus one neighbors are selected by the robust approach developed by NOTHEGGER & DORNINGER (2009). The robustness enables the estimation of planes, for example, even at walls as well as roof ridges where two planes are found in the local neighborhood, and for data with high amount of data noise or georeferencing deficiencies. The roughness is calculated for each laser point and is attached to the coordinate triple (i.e. X Y Z roughness). We implemented a GRASS GIS module that allows deriving the descriptive statistics of laser point attributes (e.g. average roughness value) for each polygon (cf. HÖFLE et al. 2008). The laser points are spatially assigned to the polygons, while the statistics are derived per polygon by using the additional columns in the point cloud file. Finally, the statistical values are written into the attribute table of the GIS vector. As mentioned above, full completeness is the major goal of the candidate region detection. Hence, solely polygons showing very high average roughness values – most probably vegetation – are rejected. Buildings where vegetation partly overlaps in 2D also have an increased average roughness but should, of course, remain. By comparing the building regions with the cadastre, a suitable threshold for average roughness is identified. All polygons having a roughness higher than 0.025 are removed from the building candidate dataset.

3.4 Building outline extraction and modeling

Accurate building outline extraction is performed best in the 3D point cloud because overhanging vegetation causes problems in the 2.5D raster domain, where these areas are most likely to be excluded from the building outline. Such a point cloud based building outline extraction method, developed by DORNINGER & PFEIFER (2008), is utilized to extract single (i.e. one but also more) building outlines within the detected candidate building regions. Firstly, data amount is reduced by selecting laser points >0.5 m above the terrain with low local roughness (see Sect. 3.3) from the entire point cloud. The outline extraction is performed sequentially for all candidate regions by extracting the laser points for each region. The applied method defines the building outline as the orthogonal projection of all roof points of a single building onto the *xy*-plane. It is initiated by a mean shift segmentation (MELZER 2007) resulting in a decomposition of the candidate point cloud into segments representing individual buildings or building parts. These segments are further subdivided into individual roof planes by means of a segmentation algorithm considering the local regression planes of the individual points. By merging roof segments belonging to one building, projecting their outline to the *xy*-plane, and finally regularizing this outline, the building outlines are derived. If none or too small roof planes are found, e.g. candidate region with solely vegetation, no building outline will be generated, which is an additional check (i.e. classification) of the candidate regions. Further details on roof outline generation and regularization are given in DORNINGER & PFEIFER (2008).

4 Results and discussion

The intermediate results of the single workflow steps have been shown above. A visual comparison of candidate regions, building outlines and cadastre is given in **Fig. 5**.

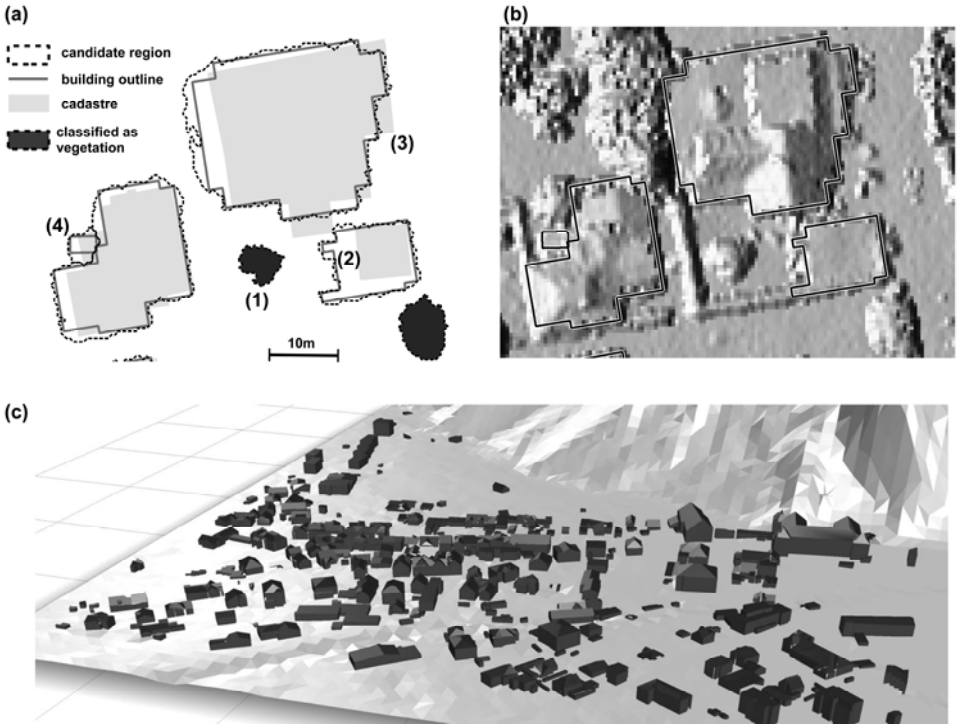

Fig. 5: (a) Comparison of detected candidate regions, modeled building outlines and digital cadastral map: (1)candidate region rejected in object-based classification, (2),(3)different representation of building in LiDAR data and cadastre, (4)oversegmentation of candidate regions; (b) shaded nDSM overlaid with final building outlines, and (c) CAD dataset of 3D building modeling output.

Error assessment is derived by intersecting the candidate regions with the DCM buildings. The candidate regions cover only 15.4% of the study area, a value very dependent on site density. However, the reduction of data volume (i.e. laser points) for following point cloud algorithms can be significant. The producer's accuracy PA (i.e. completeness) of 97.0% and the user's accuracy UA (i.e. correctness) of 72.9% show that the objective of potential building area detection can be reached with the developed method. The missing 3% completeness are mainly due to very dense trees partly covering a building, and because of the different representation of buildings in LiDAR data and cadastre (cf. RUTZINGER et al. 2009). If enough laser echoes are recorded at the occluded roof part, increasing the growing distance in the raster-based region detection or including a certain buffer around the candidate regions to select laser points could solve this problem in the point cloud based outline detection. The moderate UA can be explained by (i) vegetation regions, which could not be removed in the object-based classification and (ii) the roof overhangs, which are not included in the DCM (see **Fig. 5a,b**). The region classification procedure removes only few objects that are assumed to be vegetation. Due to the tolerant threshold for average roughness, the classification does not decrease the PA but slightly increases the UA from 71.3% to 72.9%. Currently, each detected region, even if it shares a common boundary to a

neighbor, is used independently for outline detection. By merging adjacent polygons to larger units, such effects as shown in **Fig. 5a**[(4)] can be avoided, but this requires an outline detection procedure that can find and model multiple building outlines within one candidate region. It can be expected that the final building outline polygons will significantly increase the UA, because the 3D point cloud segmentation is capable to identify and remove leftover vegetation and to delineate the objects with higher planimetric accuracy. This study does not aim at assessing the accuracy of the building outline detection algorithm (details are given in DORNINGER & PFEIFER 2008) because it is seen as exchangeable module in the whole workflow. However, the visual evaluation of the modeled building outlines shows high agreement with the building representation in the nDSM (**Fig. 5b**). A previous study by RUTZINGER et al. (2006), who derived an UA of 73% and a PA of 78% for building detection in Hohenems, shows comparable correctness. The higher completeness of our method can be explained by the strength of including the nDSM in combination with the *sER* raster for region based building detection. The nDSM allows growing the building core areas even into adjacent tree areas without overestimating the buildings where distinct edges (i.e. height jump from terrain to roof) are given.

5 Conclusions

Detection of buildings is an essential step for all applications dealing with the three-dimensional reconstruction of urban areas. This paper shows that the developed GIS workflow – making use of raster and point cloud based analysis – is capable to detect potential building regions from airborne LiDAR data with high completeness (>97%) and already moderate correctness (>70%). It is clearly stated that building outline detection and modeling has to be performed in the original LiDAR point cloud, in order to achieve the highest accuracy as well as quality. This study contributes a fast and replicable methodology to isolate building regions and to extract laser points, providing a reliable input for sophisticated building modeling applications. The developed method has only minor data requirements, as all necessary information (e.g. DTM, nDSM, Echo Ratio, surface roughness) can be derived from the plain point cloud consisting of coordinate triples (*x,y,z*). However, it is expected that new LiDAR sensors (e.g. full-waveform recording systems) with higher sampling densities and additional echo attributes (e.g. signal amplitude and echo width) will increase the accuracy of building detection and finally the quality of 3D building models.

Acknowledgments

The development of the methods presented for building outline extraction and building modeling were supported by *Vermessung Schmid* (www.geoserve.co.at) and funded by the *Christian Doppler Research Association* (www.cdg.ac.at). The LiDAR data and the digital cadastral map were kindly provided by the land survey office of Vorarlberg (*LVA Feldkirch*).

References

Dorninger, P. & Pfeifer, N. (2008), A comprehensive automated 3D approach for building extraction, reconstruction, and regularization from airborne laser scanning point clouds. Sensors 8(11), 7323 – 7343.

Filin, S. & Pfeifer, N. (2006), Segmentation of airborne laser scanning data using a slope adaptive neighborhood. ISPRS J. Photogramm. Remote Sens. 60(2), 71 – 80.

GRASS Development Team (2009), GRASS 6.4 Users Manual. Electronic document: http://grass.itc.it/grass64/manuals/html64_user/, last accessed February 2, 2009.

Höfle, B., Rutzinger, M., Geist, T. & Stötter, J. (2006), Using airborne laser scanning data in urban data management - set up of a flexible information system with open source components. – In: Proceedings of UDMS 2006. – Aalborg, Denmark, pp. 7.11 – 7.23, on CD.

Höfle, B., Hollaus, M., Lehner, H., Pfeifer, N. & Wagner, W. (2008), Area-based parameterization of forest structure using full-waveform airborne laser scanning data. – In: Proceedings Silvilaser 2008, Edinburgh, Scotland, pp. 227 – 235.

Kaartinen, H., Hyyppä, J., Gülch, E., Vosselman, G., Hyyppä, H., Matikainen, L., Hofmann, A.D., Mäder, U., Persson, Å., Söderman, U., Elmqvist, M., Ruiz, A., Dragoja, M., Flamanc, D., Maillet, G., Kersten, T., Carl, J., Hau, R., Wild, E., Frederiksen, L., Holmgaard, J. & Vester, K. (2005), Accuracy of 3d city models: EuroSDR comparison. – In: International Archives of Photogrammetry and Remote Sensing 36(3/W19), pp. 227 – 232.

Maas, H.-G. & Vosselman, G. (1999), Two algorithms for extracting building models from raw laser altimetry data. ISPRS J. Photogramm. Remote Sens. 54(2/3), 153 – 163.

Melzer, T. (2007), The mean shift algorithm for clustering point clouds. J. Appl. Geod. 1(3), 445 – 456.

Nothegger, C. & Dorninger, P. (2009), 3D filtering of high-resolution terrestrial laser scanner point clouds for cultural heritage documentation. PFG 1/2009, 51 – 62.

Pfeifer, N., Stadler, P. & Briese, C. (2001), Derivation of Digital Terrain Models in the SCOP++ Environment. – In: Proceedings of OEEPE Workshop on Airborne Laserscanning and Interferometric SAR for Detailed Digital Terrain Models. – Stockholm, Sweden, 13p.

Rutzinger, M., Höfle, B., Geist, T. & Stötter, J. (2006), Object-based building detection based on airborne laser scanning data within GRASS GIS environment. – In: Proceedings of UDMS 2006. – Aalborg, Denmark, pp. 7.37 – 7.48, on CD.

Rutzinger, M., Höfle, B. & Pfeifer, N. (2007), Detection of high urban vegetation with airborne laser scanning data. – In: Proceedings Forestsat 2007. – Montpellier, France, 5p. on CD.

Rutzinger, M., Höfle, B. & Pfeifer, N. (2008): Object detection in airborne laser scanning data - an integrative approach on object-based image and point cloud analysis. – In: Blaschke, T., Lang, S. & G. Hay (Eds.): Object-Based Image Analysis - Spatial concepts for knowledge-driven remote sensing applications. Springer Berlin.

Rutzinger, M., Rottensteiner, F. & Pfeifer, N. (2009), A comparison of evaluation techniques for building extraction from airborne laser scanning. IEEE Journal of Selected Topics in Applied Earth Observation and Remote Sensing, Vol. PP (99), 1 – 11.